Available online at www.sciencedirect.com

SciVerse ScienceDirect

Procedia Environmental Sciences 13 (2012) 2031 – 2044

Procedia Environmental Sciences

The 18th Biennial Conference of International Society for Ecological Modelling

Assessment on water use efficiency under climate change and heterogeneous carbon dioxide in China terrestrial ecosystems

Z. Zhang[a], H. Jiang[ab*], J.X. Liu[c], G.M. Zhou[b], S.R. Liu[d], X.Y. Zhang[a]

[a]*International Institute for Earth System Science, Nanjing University, Hankou Road 22, Nanjing 210093, China*
[b]*State Key Laboratory of Subtropical Forest Science & Zhejiang Provincial Key Laboratory of Carbon Cycling in Forest Ecosystems and Carbon Sequestration, Zhejiang Agriculture and Forestry University, Hangzhou, 311300, Zhejiang, China*
[c]*Stinger Ghaffarian Technologies (SGT, Inc.), contractor to the U.S. Geological Survey (USGS) Earth Resources Observation and Science (EROS) Center, 47914 252nd St., Sioux Falls, SD 57198. Work performed under USGS contract G10PC00044.*
[d]*Institute of Forest Ecology and Environment, Chinese Academy of Forestry, Beijing 100091, China.*

Abstract

Assessing the effects of climate change on water use efficiency (WUE) is critical for policymaking and adaptation. The influences of heterogeneous distribution of atmospheric carbon dioxide (CO_2) concentration on WUE have not considered in China. In this study, we used a spatial-temporal distribution of CO_2 constructed from remote sensing data and ground-based observations, to quantify the heterogeneity of CO_2 concentrations. Based on the initial conditions, the spatial patterns of WUE in history and future were estimated using the Integrated Biosphere Simulator (IBIS). Results showed that the geographical distributions of the averaged WUE have significant difference under the heterogeneous surface CO_2 fertilization condition during 1951-2006. Partial correlation analysis indicated that the cold temperate zones are strong associated with the spatial heterogeneity of CO_2, suggesting the special relationship of carbon-water cycle coupling with the interannual variations of CO_2. WUE showed high negative correlations with temperature in subtropical zones and positive correlations in Tibet Plateau. The correlation between WUE and precipitation exhibits high positive in wet temperate zones, where the cropland is mainly located. Our estimates of WUE and its covariation with major climate variables can improve understanding of carbon-water cycle coupling under climate change.

Keywords: water use efficiency; CO_2 fertilization; Atmospheric CO_2 concentration; IBIS; climate change

* Corresponding author. Tel.: +86-25-83595969; fax: +86-25-83592288.
E-mail address: jianghong_china@hotmail.com.

 doi:10.1016/j.proenv.2012.01.194

1. Introduction

China is a country significantly diverse in ecosystem types and climate zones: from coastal ecosystem to desert ecosystem and from tropical to cold temperate. Moreover, due to the rapid economic development, the distribution patterns of CO_2 concentration have been influenced by anthropogenic Green House Gas (GHG) emission and thus have great effect on the carbon and water cycles of terrestrial ecosystems in China. However, it is unclear how and to what extent the climate change and spatial-temporal heterogeneity of CO_2 have affected the carbon and water cycles.

Water Use Efficiency (WUE), a key measurement for the carbon and water cycle coupling function of terrestrial ecosystems, is used to describe the trade-off between water loss and carbon sequestration in the process of plant photosynthesis carbon assimilation [1]. WUE can enhance our ability to predict how climate change may affect the carbon and water budgets [2]. On the other hand, Atmospheric carbon dioxide (CO_2) concentration increase and its fertilization effects are topics of serious concern in global climate change research [3]. It is essential to predict how WUE of different plants would respond to the environmental and increasing atmospheric CO_2 levels [4].

Numerous experimental studies performed to date revealed that CO_2 enhancement not only increase plant biomass, but also positively affect WUE and nitrogen use efficiency [5-7]. However, these controlled experiments (i.e. open-top chamber (OTC), free air carbon dioxide enrichment (FACE)) quantify the responses of plants species to CO_2 enrichment in the small scale, and there is no study on spatial-temporal heterogeneity of CO_2 enrichment due to inadequate measurement techniques.

Beginning in the early 2000s, large-area CO_2 monitoring developed with remote sensing technology. The Scanning Imaging Absorption Spectrometer for Atmospheric Cartography (SCIAMACHY) of ENVISAT [8] and the Greenhouse Gases Observing Satellite (GOSAT) [9], provide spatial and temporal heterogeneity measures of CO_2 that represent dry air average column value of atmospheric CO_2. Ground-based stations that continually measure the land surface CO_2 concentration of different ecosystems also provide temporal variations globally [10]. For filling the gap between ground and remote sensing data and evaluation historical and future CO_2 patterns, a sine wave and linear coupled model was established to reconstruct the spatial distributions of historical and future CO_2 concentration.

Although the eddy covariance technique, as a widely used measurement technique, is a powerful tool to evaluate WUE at ecosystem level [11-13], it could not forecast future situation and is difficult to evaluate WUE at larger level. To avoid these limitations, an integrated biogeochemical model, the Integrated Biosphere Simulator (IBIS), was coupled with spatial distributions of historical and future CO_2 concentration to study the temporal-spatial dynamic of WUE at large scale. The IBIS model includes a land-process module and a plant physiological module, and is adapted to extrapolate current knowledge to a larger scale both in space and time [14,15].

In this study, WUE was calculated as the ratio of net primary productivity (NPP) to evaportranspiration (ET), a definition widely adopted to estimate the WUE at regional level [16,17]. A well-evaluated integrated ecosystem model (IBIS) and constructed historical-future data of surface CO_2 concentration were used to simulate the spatial and temporal changes of WUE under climate change. Our objectives were to assess: (1) the spatial patterns of WUE under spatial heterogeneity of CO_2 enrichment; (2) the impacts of climate change factors (temperature, precipitation, rising atmospheric concentration) on spatial distributions of WUE; (3) future trend of WUE under IPCC climate change scenarios.

2. Materials and methods

2.1. Model Description

The IBIS model is designed as an integrated, physically consistent modeling framework which includes land surface processes, canopy physiology, vegetation phenology long-term vegetation dynamics, and carbon cycling. Detailed IBIS model descriptions are available in [18] and [14]. However, this original model does contain a complete nitrogen (N) cycle. A modified version of IBIS was developed to overcome this limitation [19].

The canopy physiology module included photosynthesis and stomatal conductance, which were based on a canopy photosynthesis mechanism model and a semi-mechanistic model of stomatal conductance [20]. The NPP calculation differed from each other in different plant functional types:

$$NPP = (1-\eta)\int (A_g - R_a)dt \quad (1)$$

where A_g was gross canopy photosynthesis, R_a was the rate of gross plant respiration.
For C_3 plants:

$$A_g \approx \min(J_e, J_c) \quad (2)$$

where J_E was the light limited rate of photosynthesis, Jc was the Rubisco limited rate of photosynthesis.
For C4 plants:

$$A_g \approx \min(J_I, J_E, J_C) \quad (3)$$

where $J_E = \alpha_4 Q_p$ was the intrinsic quantum efficiency for CO_2 uptake in C_4 plant (mol CO_2 Ein^{-1}), and J_c, J_l was the CO_2 limited rate of photosynthesis at low-CO_2 concentrations.

The hydrological module is constructed based on a land-surface-transfer scheme (LSX) [21,22]. This module applied two canopy layers, three snow layers, and six soil layers to construct land surface physically. The total amount of evaportranspiration from the land surface is calculated as the sum of three water vapor fluxes: canopy transpiration, evaporation of water intercepted by vegetation canopies, evaporation from the soil surface. Evaporation rates are calculated using standard mass transfer equations relating the temperature of the surface, vapor pressure deficit, and conductance [23].

2.2. Study area and data

In this study, climate zones, categorized into 11 major regions by using basic meteorological principles (temperature and moisture), were used to analysis the different responses of WUE under different climate and geographical conditions in China (Fig. 1). IBIS simulation in China was performed at 0.085-degree (~ 10-km) resolution. Fundamental data of simulation were collected from Zhu et al., 2010. In addition, Vegetation cover fractions, initial biomass carbon, initial soil carbon, soil texture, topography, and monthly climate data were interpolated to ensure consistency. Vegetation cover fractions were calculated from the 300-m resolution GLC map. Initial biomass was derived from Olson's World Ecosystem database [24]. Initial soil information was obtained from the IGBP global database [25]. Atmospheric nitrogen deposition data were acquired from the Earth Science Information Partner (ESIP) database of the EOS-WEBSTER, which covers the early 1990s. The CGCM3 future climate data (IPCC SRES A2 and B1 scenarios) were obtained from the Canadian Centre for Climate Modeling and Analysis (CCCma) (http://www.ec.gc.ca/ccmac-cccma).

The trend of CO_2 increase was consistent with historical observation and future IPCC scenarios. The historical period (1901 to 2008) was derived from ESRL, while the future trends were based on ISAM model [26]. The two scenarios represent different CO_2 emission level. The CO_2 concentrations will

increase to 850 ppm under the A2 scenario and 540 ppm under the B1 scenario. All the CO_2 concentration data were fitted by a double exponential curve so that the fitted parameters can be used in double and exponential model.

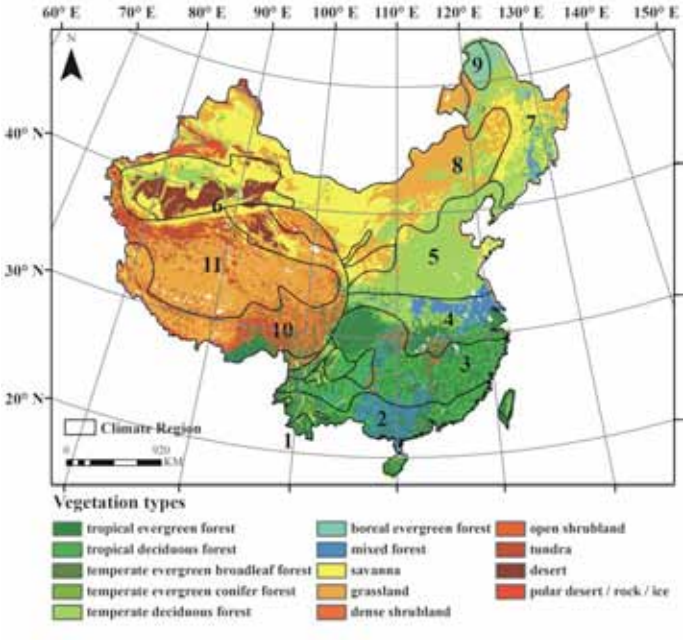

Fig. 1 Vegetation type map and the geographical delineation of climate zones in China: 1) Marginal Tropical (MT); 2) Southern Subtropical (SS); 3) Middle Subtropical (MS); 4) Northern Subtropical (NS); 5) WetWarm Temperate (WWT); 6) DryWarm Temperate (DWT); 7) WetMiddle Temperate (WMT); 8) DryMiddle Temperate (DMT); 9) Cold Temperate (CT); 10) Plateau Temperate (PT); 11) Plateau Frigid (PF).

2.3. Spatial-temporal patterns of atmospheric CO_2 concentration

In situ measurements of atmospheric CO_2 concentration are obtained at GAW field stations worldwide. The spatial-temporal heterogeneity of atmospheric CO_2 concentration has been detected from these ground-based CO_2 measurement networks [27]. Since 2000s, Monitoring atmospheric CO_2 concentration using satellite became a reliable technology for representing the spatial and temporal variability of CO_2 globally [28]. However, The CO_2 column observation of remote sensing cannot represent surface CO_2 concentration. Therefore, a set of linear regression equations between the SCIAMACHY CO_2 column and the GAW-observed surface CO_2 was developed for major vegetation types to estimate the spatially heterogeneous land surface CO_2 concentrations worldwide. The square regression coefficients were significant, indicating the linear model results were reliable (Appendix A1).

Land surface CO_2 concentration is influenced by vegetation uptake, fossil fuel emissions, ocean uptake, wildfire and other land cover and land use disturbances, and CO_2 transportation [29]. Hence the CO_2 concentration has a periodic variation due to plant phenological variations. From analysis of GAW monthly results, a combined double exponential function and a sine wave function were developed to represent the temporal pattern of increasing and periodic CO_2 trend:

$$Y_t = \left(A + e^{B*X_t} + e^{C*X_t}\right) + E \sin\left(2\frac{\pi}{F}X_t + G\right) + H \qquad (4)$$

where Y_t is the land surface CO_2 concentration; X_t is monthly time, starting from January 1991. The first term represents the overall long-term CO_2 trends. A, B, and C are the regression parameters (Appendix A1) for the double exponential CO_2 trend line. The second term describes the annual periodic feature of CO_2 with the parameters E, F, G, and H representing wavelength, period, phase adjustment, and the residue of estimated surface CO_2 and observed value, respectively. The E, F, G, and H parameters are specific to different vegetation types (Appendix A2).

2.4. Simulation setup and model validation

Six model simulations were performed: (1) A2 with heterogeneous CO_2 increase, (2) A2 with uniform CO_2 increase, (3) B1 with heterogeneous CO_2 increase, (4) B1 with uniform CO_2 increase, (5) A2 with no CO_2 increase, and (6) B1 with no CO_2 increase.

Simulation (1) and (3), with CO_2 enrichment and spatial variability, denoted as CO_2-E, are to be compared with the simulations of CO_2 enrichment but no spatial variability (2) and (4), denoted as CO_2-B, in order to quantify the potential impacts of spatially heterogenic distribution of CO_2 on C sequestration. Simulation (5) and (6), denoted as CO_2-N, are mainly used to quantify the impacts of CO_2 increase on C sequestration with simulation (2) and (4). By comparing the six model simulations, the effects of CO_2 fertilization and heterogeneous CO_2 enrichment can be quantified (Table 1).

Table 1. Conditions of each simulation experiment

No.	Scenarios& Climate data	CO_2 concentration (2050)	CO_2 concentration (2099)	CO_2 increase type
1	A2 & CO_2-E A2	532 (ISAMS)	856 (ISAMS)	Spatial- variations, monthly
2	A2&CO_2-B A2	532 (ISAMS)	856 (ISAMS)	Non Spatial- variations, yearly
3	B1 & CO_2-E B1	488 (ISAMS)	549 (ISAMS)	Spatial- variations, monthly
4	B1& CO_2-B B1	488 (ISAMS)	549 (ISAMS)	Non Spatial- variations, yearly
5	A2&CO_2-N A2	305ppm(1901 level)	305ppm	No increase
6	B1&CO_2-N B1	305ppm(1901 level)	305ppm	No increase

Model simulations were from 1901 to 2099. The spin-up period was from simulated 1901 to 1950 (using 1951–2000 average climate condition). This period allowed the ecosystem carbon pool and vegetation structures to reach a relative equilibrium. Simulation results from 1951 to 2099 were analyzed.

IBIS has been widely applied at different scales and in different regions for carbon and hydrological cycling investigation [15,18]. In China, the evaluation of IBIS model on water cycling was performed [30]. For carbon cycling process, net primary production and biomass were validated with forestry inventory data [31]. The IBIS simulated total carbon sequestration and exchange of China were compared with literature report data (my MS). The validation showed reasonable agreement.

2.5. WUE calculation

Based on different scales and approaches, WUE has different meanings because of the different complexity of physical and physiological processes involved. Some new methods such as eddy covariance technique were applied to calculate WUE using the ratio of GPP to ET [32]. At ecosystem level, the ratio of above-ground net primary productivity (ANPP) to precipitation was used to replace ET

to calculate precipitation use efficiency [33]. NPP/ET was also a major definitions used in many studies [16]. In this study, the NPP-based WUE was used to address the objective since NPP reflect annual net carbon fixation and plant biomass.

3. Results

3.1. The spatial-temporal pattern of CO_2 concentration

For the spatial pattern of CO_2 concentration, simulated CO_2 concentration in northwestern China is always lower than in eastern and southern China (Fig.2b).The CO_2 concentration of northeastern China is also lower than average level. The average difference is about $\pm$20ppm. The extreme difference between some locations can be as big as $\pm$30 ppm. The high CO_2 concentration regions are mainly located at southeast and central of China. The monthly variations of each climate zones showed different pattern both in annual average value and inter-annual magnitude (Fig.2a).The DWT zone had the lowest mean yearly value of CO_2 concentration, while the NS, MS zones has about 4 ppm higher than other regions. The CT zone, which was mainly covered by boreal forest, has the highest magnitude in China. This indicated that the inter-annual variations of CO_2 in CT zone was more sensitive to periodic change.

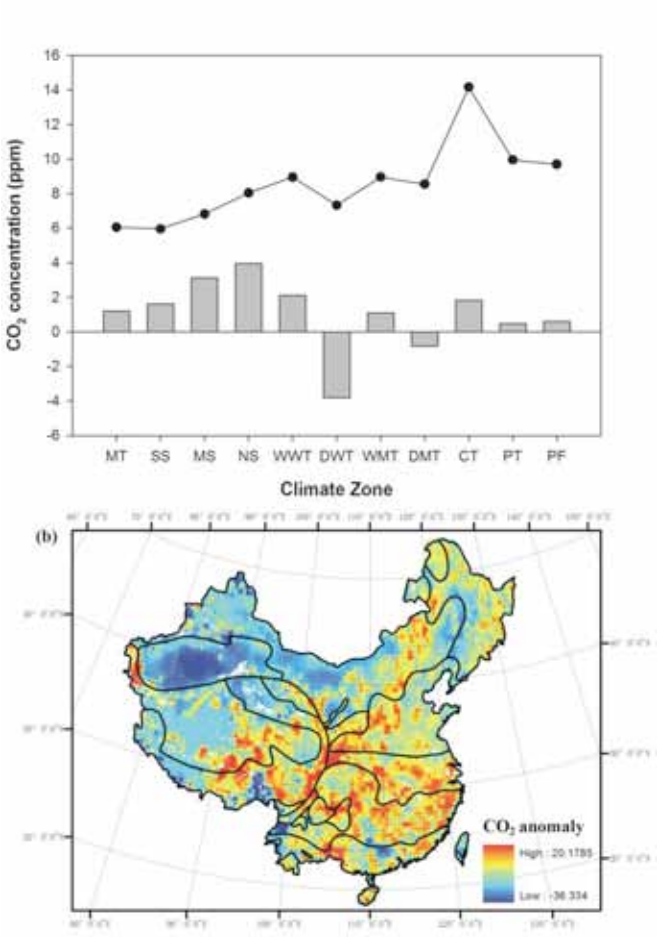

Fig.2 Modeled spatial anomaly of surface CO_2 concentration in China using satellite data and ground-based observation (my MS). a, Anomaly of mean CO_2 concentration across different climate zones in China. Dotted line represents the inter-annual magnitude of mean CO_2 concentration in each climate zones. The vertical bars show the mean deviation of CO_2 differences respect to the annual global average level. b, Spatial pattern of monthly CO_2 concentration anomaly in China.

3.2. Spatial patterns of WUE under different CO_2 enrichment condition

The spatial pattern of yearly averaged WUE from 1951 to 2000 is shown in Fig.3a. The highest WUE was in the southeast of China with 0.8-1.0 g C/kg H_2O, while the lowest value was found in the northwestern China, which was covered by bare area. In most areas of Qinghai-Tibet Plateau, WUE was about 0.3-0.5 g C/kg H_2O. Due to the geographical differences and surface climate conditions, WUE had a significant spatial diversity in the regions of China.

Under CO_2 enrichment effect with spatial heterogeneous conditions, WUE has considerable differences comparing to the CO_2 uniform pattern (Fig.3b), albeit of little amounts in some regions. In southeastern China, WUE was 0.02 g C/kg H_2O higher than the reference CO_2-B simulation. This

indicates that the CO_2 spatial heterogeneity produced a constantly higher WUE than former estimated on the large regional scale. There was also an increase in WUE in the northeast and central of China, which was ranged from 0.01-0.15 g C/kg H_2O. Besides the positive effect of CO_2 spatial heterogeneity on WUE, the slightly negative effect was present in some southern area of Qinghai-Tibet Plateau. In northwestern China covered with sparse vegetation, there was little differences on WUE. In overall, heterogeneous CO_2 enrichment has a significant effect on WUE, and the magnitude of this enhancement effect depend in part on CO_2 concentration pattern as well as vegetation cover types.

Comparing the geographical distribution of WUE for the period of 1951 to 2000 between the CO_2-E simulation to the CO_2-N simulation, the map showed CO_2 enrichment effects on WUE in China (Fig.3c). In southeastern and northeastern China, where was mainly covered by temperate and boreal forest, CO_2 enrichment has positive effect on WUE with a range from 0.07 to 0.1 g C/kg H2O. Similar increasing pattern was found in Qinghai-Tibet Plateau, where was covered with plateau meadow. CO_2 enrichment has no obvious effect on WUE in the northwestern China, because desert and bare areas were dominated in these regions. This indicated that the CO_2 enhancement effect on WUE was to a large extent attributed to the land vegetation cover.

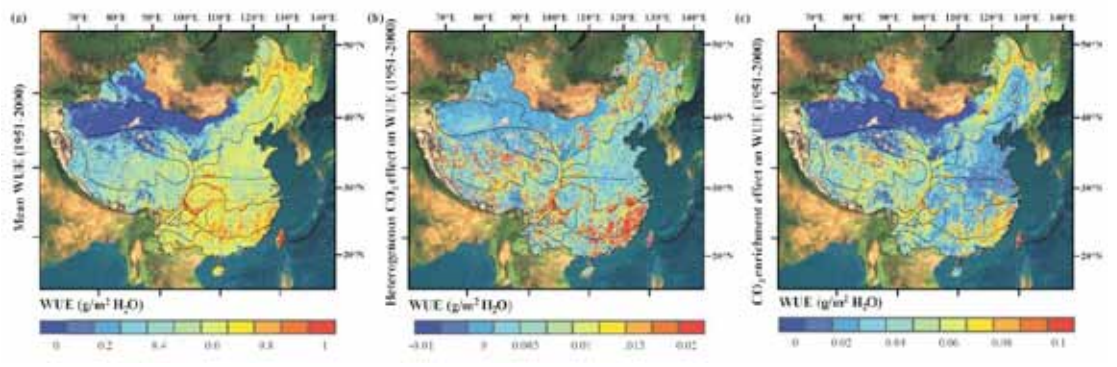

Fig.3 Spatial distribution of mean annual WUE (a), heterogeneous CO_2 effect on WUE (b) and CO_2 enrichment effect on WUE (c) across the terrestrial ecosystems of China from 1951-2000. Heterogeneous CO_2 effect on WUE was calculated using the subtraction between CO_2-E simulation subtract CO_2-B simulation, CO_2 enrichment effect on WUE was represented as the subtraction between CO_2-E simulation and CO_2-N simulation.

3.3. Influences of climate change on WUE

To consider the effects of temperature, precipitation and rising CO_2 concentration on WUE, A further partial correlation in the spatial pattern between WUE and these climate change factors was introduced (Fig. 4).

Strong negative correlations were shown (< -0.6) between the annual WUE and mean annual temperature in southern China, where was mainly categorized into MT, SS, MS. Among climate zones PT and PF, significant positive correlations were found between the annual WUE and temperature, and slightly positive correlations were shown in the west areas of DMT. In other climate zone, there was no significant correlation between the annual WUE and temperature.

For the relationship between annual WUE and precipitation, the spatial pattern of partial correlation coefficient appeared different from that of temperature. Precipitation has a significant positive effect on

the ecosystems in the climate zones NT, WWT, where vegetation is mainly cropland. There was an opposite pattern in PT, PF and some areas of DMT, indicating that precipitation has a significant negative correlation with WUE. This result could be probably associated with the large sparse vegetation covered in these regions, because ET in these regions would be overestimated when precipitation increased. WUE had no significant correlation with rising CO_2 concentration in most areas of China (Fig.4c), but it did in some important climate zones such as CT SS and MS. High correlations between WUE and CO_2 concentration were found in these regions.

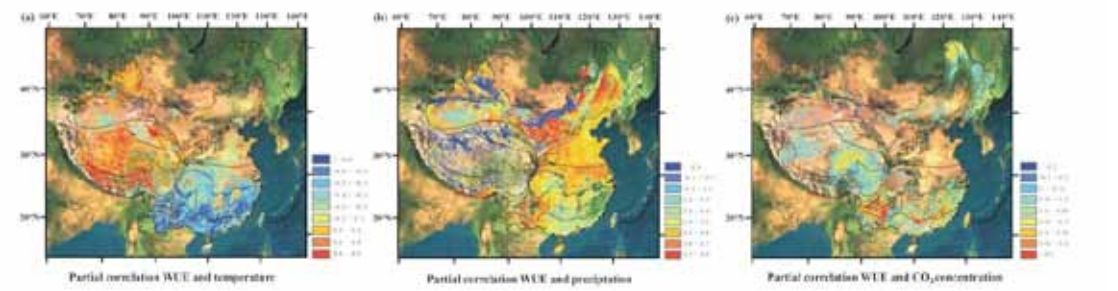

Fig.4 Partial correlation in the spatial domain between WUE and temperature, precipitation, or CO_2 concentration. Shown are significant correlations ($p<0.01$) of which the correlation coefficient is higher/lower than ±0.2.

4. Discussion & Conclusion

4.1. Importance of CO_2 Enrichment on WUE

Many studies have proved that rising atmospheric CO_2 concentration did increase WUE over the last century, whatever the research techniques applied (e.g. FLUXNET, field experiments, model) [5,16,33,34]. In the view of plant physiology, this enhancement is performed through a decrease in stomatal conductance and an increase in photosynthesis rate [35]. These influences will propose as the trade-off between the amount of carbon assimilated and the amount of water transpired [36]. Although CO_2 is a rapid-mixing gas in atmosphere, the spatial heterogeneity of land surface CO_2 concentration are exist due to the even severe anthropogenic emission and will be more significant in future. The spatial and temporal heterogeneity of CO_2 provided by satellite observation will consequently have an influence on carbon and water cycles of terrestrial ecosystems of China. As the IBIS model results indicated, the mean WUE in China under spatial-temporal heterogeneity of CO_2 is higher than that of uniform CO_2 pattern. Considering the different productivity abilities and geographies conditions among different ecosystem, we found that there is an underestimation of WUE in subtropical regions and an overestimation of WUE in tropical regions. Meanwhile, the WUE in boreal forest and cold temperate zones is sensitive to the rising and inner-variation of CO_2 concentration.

4.2. Impact of Climate change coupled CO_2 enrichment

Table 2. Percentage of area for which WUE is climatically dominated, indicated by a partial correlation coefficient higher than 0.2 (or 0.5 in brackets). Historical climate grids (temperature and precipitation) and CO_2 spatial-temporal grids were used to perform a partial correlation between the WUE and climate variables. Then, the fractional area with significant ($p < 0.01$) partial correlation higher than 0.2 (0.5) was calculated. (T, P represents temperature and precipitation respectively)

Climate Zone	T dominated	P dominated	CO_2 dominated
Marginal Tropical	86(36)	77(33)	35(1)
Southern Subtropical	93(49)	67(23)	64(6)
Middle Subtropical	84(29)	65(22)	43(5)
Northern Tropical	62(5)	82(62)	15(1)
Wet Warm Temperate	25(3)	88(67)	9(1)
Dry Warm Temperate	19(0)	73(25)	15(0)
Wet Middle Temperate	4(0)	50(22)	35(0)
Dry Middle Temperate	24(0)	83(51)	14(1)
Cold Temperate	6(0)	0(0)	97(0)
Plateau Temperate	53(8)	48(14)	36(0)
Plateau Frigid	57(2)	37(9)	38(0)

Under the impact of climate change and rising CO_2 concentration, the globally WUE has been totally affected [37]. However, the present researches are focus on at ecosystem level or lower level. For the spatial variations of WUE and its spatial responses to climate change, there are few researches deal with climate change and spatially heterogeneous CO_2. Actually, it is important to evaluate the controlling factors of climate change on WUE under a more reality of world. Understanding the spatial pattern of WUE and its environmental control mechanisms is of great significance for assessing the ecosystem carbon budget and for evaluating the water carrying capacity of ecosystems and its variation under changing climate. The three environmental factors dominated a wide range of China (Table 2). Although they may not represent all controlling valuables in climate change, this study provides valuable information for investigating the effects of climate change on terrestrial ecosystems WUE of China.

As temperature decreased when latitude and elevation increased, the WUE has significant relationship with precipitation. Most areas of the region which was dominated by precipitation were covered by cropland. Climate change with increasing precipitation may optimize the water resource condition, which would increase the yield of the plants. Meanwhile, it seemed that CO_2 concentration has great effects in boreal forest and cold temperate zones. On the other hand, with rising CO_2 concentration, increasing WUE will enhance the resistance to drought in these regions. By combining recent research on atmospheric CO_2 in high latitude regions with our model results, we believe that it is essential to further study the inner relationship between annual WUE and seasonal variations of CO_2 concentration in boreal forest and cold temperate zones, especially under the more ever extreme climate events nowadays.

Acknowledgements

Funding support partially from The State Key Fundamental Science Funds of China (2010CB950702 and 2010CB428503), The State High Technology Funds of China (2009AA122001 and 2009AA122005), The State Key International Cooperation Project (20073819), The State Key Basic Research Funds of China (2007FY110300-04 & 08), NSF-China Project (40671132 & 30590383), and The key project of Zhejiang Province (2008C13G2100010). Any use of trade, product, or firm names is for descriptive purposes only and does not imply endorsement by the U.S. Government.

References

[1] Baldocchi D, A Comparative-Study of Mass and Energy-Exchange Rates over a Closed C_3 (Wheat) and an Open C_4 (Corn) Crop .2. CO_2 Exchange and Water-Use Efficiency, *AGR FOREST METEOROL*, 1994, **67 (3-4)**: 291-321.

[2] Hu Z, Yu G, Fu Y, Sun X, Li Y, Shi P, Wang Y, Zheng Z, Effects of vegetation control on ecosystem water use efficiency within and among four grassland ecosystems in China, *GLOB CHANGE BIOL*, 2008, **14 (7)**: 1609-19.

[3] Heimann M, Reichstein M, Terrestrial ecosystem carbon dynamics and climate feedbacks, *Nature*, 2008, **451 (7176)**: 289-92.

[4] Law BE, Falge E, Gu L, Baldocchi DD, Bakwin P, Berbigier P, Davis K, Dolman AJ, Falk M, Fuentes JD, Goldstein A, Granier A, Grelle A, Hollinger D, Janssens IA, Jarvis P, Jensen NO, Katul G, Mahli Y, Matteucci G, Meyers T, Monson R, Munger W, Oechel W, Olson R, Pilegaard K, Paw KT, Thorgeirsson H, Valentini R, Verma S, Vesala T, Wilson KWofsy S, Environmental controls over carbon dioxide and water vapor exchange of terrestrial vegetation, *AGR FOREST METEOROL*, 2002, **113 (1-4)**: 97-120.

[5] Peñuelas J, Canadell JG, Ogaya R, Increased water-use efficiency during the 20th century did not translate into enhanced tree growth, *GLOBAL ECOL BIOGEOGR* , 2010, **20 (4)**: 597-608.

[6] Andreu-Hayles L, Planells O, GutiÉRrez E, Muntan E, Helle G, Anchukaitis KJSchleser GH, Long tree-ring chronologies reveal 20th century increases in water-use efficiency but no enhancement of tree growth at five Iberian pine forests, *GLOB CHANGE BIOL*, 2010, **17 (6)**: 2095-112.

[7] Garbulsky MF, Penuelas J, Papale D, Ardo J, Goulden ML, Kiely G, Richardson AD, Rotenberg E, Veenendaal EMFilella I, Patterns and controls of the variability of radiation use efficiency and primary productivity across terrestrial ecosystems, *GLOBAL ECOL BIOGEOGR* , 2010, **19 (2)**: 253-67.

[8] Schneising O, Buchwitz M, Burrows J, Bovensmann H, Reuter M, Notholt J, Macatangay RWarneke T, Three years of greenhouse gas column-averaged dry air mole fractions retrieved from satellite Part 1: Carbon dioxide, *Atmos. Chem. Phys.*, 2008, **8**: 3827-53.

[9] Yokota T, Yoshida Y, Eguchi N, Ota Y, Tanaka T, Watanabe H, Maksyutov S, Global Concentrations of CO_2 and CH_4 Retrieved from GOSAT: First Preliminary Results, *SOLA*, 2009, **5 (0)**: 160-3.

[10] Peters W, Krol MC, Van Der Werf GR, Houweling S, Jones CD, Hughes J, Schaefer K, Masarie KA, Jacobson AR, Miller JB, Cho CH, Ramonet M, Schmidt M, Ciattaglia L, Apadula F, Heltai D, Meinhardt F, Di Sarra AG, Piacentino S, Sferlazzo D, Aalto T, Hatakka J, StrÖM J, Haszpra L, Meijer HAJ, Van Der Laan S, Neubert REM, Jordan A, RodÓ X, MorguÍ JA, Vermeulen AT, Popa E, Rozanski K, Zimnoch M, Manning AC, Leuenberger M, Uglietti C, Dolman AJ, Ciais P, Heimann MTans PP, Seven years of recent European net terrestrial carbon dioxide exchange constrained by atmospheric observations, *GLOB CHANGE BIOL*, 2010, **16 (4)**: 1317-37.

[11] Yu GR, Song X, Wang QF, Liu YF, Guan DX, Yan JH, Sun XM, Zhang LM, Wen XF, Water-use efficiency of forest ecosystems in eastern China and its relations to climatic variables, *NEW PHYTOL* , 2008, **177 (4)**: 927-37.

[12] Pingintha N, Leclerc MY, Beasley JP, Durden D, Zhang G, Senthong C, Rowland D, Hysteresis response of daytime net ecosystem exchange during drought, *BIOGEOSICENCES*, 2010, **7 (3)**: 1159-70.

[13] Jassal R, Black T, Spittlehouse D, Br¨¹mmer CNesic Z, Evapotranspiration and water use efficiency in different-aged Pacific Northwest Douglas-fir stands, *AGR FOREST METEOROL*, 2009, **149 (6-7)**: 1168-78.

[14] Foley JA, Prentice IC, Ramankutty N, Levis S, Pollard D, Sitch S, Haxeltine A, An integrated biosphere model of land surface processes, terrestrial carbon balance, and vegetation dynamics, *GLOBAL BIOGEOCHEM CY* , 1996, **10 (4)**: 603-28.

[15] Cramer W, Bondeau A, Woodward FI, Global response of terrestrial ecosystem structure and function to CO_2 and climate change: results from six dynamic global vegetation models, *GLOB CHANGE BIOL*, 2001, **7**: 357-73.

[16] Tian HQ, Chen GS, Liu ML, Zhang C, Sun G, Lu CQ, Xu XF, Ren W, Pan SF, Chappelka A, Model estimates of net primary productivity, evapotranspiration, and water use efficiency in the terrestrial ecosystems of the southern United States during 1895-2007, *FOREST ECOL MANAG*, 2010, **259 (7)**: 1311-27.

[17] Bai Y, Wu J, Xing Q, Pan Q, Huang J, Yang D, Han X, Primary production and rain use efficiency across a precipitation gradient on the Mongolia plateau, *ECOLOGY*, 2008, **89**: 2140-53.

[18] Kucharik CJ, Foley JA, Delire C, Fisher VA, Coe MT, Lenters JD, Young-Molling C, Ramankutty N, Norman JMGower ST, Testing the performance of a Dynamic Global Ecosystem Model: Water balance, carbon balance, and vegetation structure, *GLOBAL BIOGEOCHEM CY* , 2000, **14 (3)**: 795-825.

[19] Liu JX, Price DT, Chen JA, Nitrogen controls on ecosystem carbon sequestration: a model implementation and application to Saskatchewan, Canada, *ECOL MODEL* , 2005, **186 (2)**: 178-95.

[20] Farquhar GD, Sharkey TD, Stomatal Conductance and Photosynthesis, *ANNU REV PLANT PHYS* , 1982, **33 (1)**: 317-45.

[21] Thompson SL, Pollard D, A Global Climate Model (Genesis) with a Land-Surface Transfer Scheme (Lsx) .1. Present Climate Simulation, *J CLIMATE* , 1995, **8 (4)**: 732-61.

[22] Thompson SL, Pollard D, A Global Climate Model (Genesis) with a Land-Surface Transfer Scheme (Lsx) .2. CO_2 Sensitivity, *J CLIMATE* , 1995, **8 (5)**: 1104-21.

[23] Campbell GS, Norman JM, *An Introduction to Environmental Biophysics*. 1998: Springer-Verlag. 286.

[24] Gibbs H, Olsen L, Boden T, Major World Ecosystem Complexes Ranked by Carbon in Live Vegetation: An Updated Database Using the GLC2000 Land Cover Product, *Oak Ridge National Laboratory, Oak Ridge, USA*, 2006.

[25] Task G, Global gridded surfaces of selected soil characteristics (IGBP-DIS), *International Geosphere-Biosphere Programme-Data and Information Services. Available on-line [http://www. daac. ornl. gov/] from Oak Ridge National Laboratory Distributed Active Archive Center, Oak Ridge, Tennessee, USA*, 2000.

[26] Jain AK, Wuebbles DJ, Kheshgi HS, *Integrated science model for assessment of climate change*. 1994. Medium: ED; Size: 19 p.

[27] Zhang D, Tang J, Shi G, Nakazawa T, Aoki S, Sugawara S, Wen M, Morimoto S, Patra PHayasaka T, Temporal and spatial variations of the atmospheric CO_2 concentration in China, *GEOPHYS RES LETT* , 2008, **35 (3)**: L03801.

[28] Buchwitz M, Schneising O, Burrows J, Bovensmann H, Reuter M, Notholt J, First direct observation of the atmospheric CO_2 year-to-year increase from space, *Atmos. Chem. Phys*, 2007, **7**: 4249-56.

[29] Peters W, Jacobson A, Sweeney C, Andrews A, Conway T, Masarie K, Miller J, Bruhwiler L, P¨¦tron G, Hirsch A, An atmospheric perspective on North American carbon dioxide exchange: CarbonTracker, *P NATL ACAD SCI USA* , 2007, **104 (48)**: 18925.

[30] Zhu Q, Jiang H, Liu J, Wei X, Peng C, Fang X, Liu S, Zhou G, Yu SJu W, Evaluating the spatiotemporal variations of water budget across China over 1951-2006 using IBIS model, *HYDROL PROCESS* , 2010, **24 (4)**: 429-45.

[31] Zhu Q, Jiang H, Peng C, Liu J, Wei X, Fang X, Liu S, Zhou G, Yu S, Evaluating the effects of future climate change and elevated CO_2 on the water use efficiency in terrestrial ecosystems of China, *ECOL MODEL* , 2011, **222 (14)**: 2414-29.

[32] Li JH, Erickson JE, Peresta G, Drake BG, Evapotranspiration and water use efficiency in a Chesapeake Bay wetland under carbon dioxide enrichment, *GLOB CHANGE BIOL*, 2010, **16 (1)**: 234-45.

[33] Hu Z, Yu G, Fan J, Zhong H, Wang S, Li S, Precipitation-use efficiency along a 4500-km grassland transect, *GLOBAL ECOL BIOGEOGR* , 2010, **19 (6)**: 842-51.

[34] Brienen R, Wanek W, Hietz P, Stable carbon isotopes in tree rings indicate improved water use efficiency and drought responses of a tropical dry forest tree species, *TREES-STRUCT FUNCT* , 2011, **25 (1)**: 103-13.

[35] Farquhar GD, Caemmerer S, Berry JA, A biochemical model of photosynthetic CO_2 assimilation in leaves of C_3 species, *Planta*, 1980, **149 (1)**: 78-90.

[36] Farquhar GD, Carbon dioxide and vegetation, *Science*, 1997, **278** (5342): 1411.

[37] Beer C, Ciais P, Reichstein M, Baldocchi D, Law BE, Papale D, Soussana JF, Ammann C, Buchmann N, Frank D, Gianelle D, Janssens IA, Knohl A, Kostner B, Moors E, Roupsard O, Verbeeck H, Vesala T, Williams CA, Wohlfahrt G, Temporal and among-site variability of inherent water use efficiency at the ecosystem level, *GLOBAL BIOGEOCHEM CY* , 2009, **23**: GB2018.

Appendix A. spatial-temporal pattern of CO_2 concentration

A.1. Vegetation types in IBIS and their parameters of sine function calculated from GAW sites

By applying the sine function to the categorized GAW stations (by vegetation type), our results showed most of the r2 values to be above 0.9, indicating the sine function is suitable for representing the CO_2 periodic dynamics.

Table Vegetation types in IBIS and their parameters of sine function calculated from GAW sites.

Vegetation type	E	F	G	H	GAW Sites
tropical evergreen forest	2.496	12.81	-1.364	2.804	DMV, BKT
tropical deciduous forest	2.879	11.99	0.513	1.384	KUM,KEY
temperate evergreen broadleaf forest	3.605	11.78	2.082	2.433	LLN,SSL
temperate evergreen conifer forest	4.452	11.96	-1.677	2.362	ESP,HAT
temperate deciduous forest	8.285	11.99	2.477	2.916	NGL,HPB
boreal evergreen forest	6.914	12.02	2.866	2.367	CDL,ETL
savanna	2.103	12.98	1.727	1.239	DIG,KPS
grassland	4.175	11.99	-3.111	1.322	MKN,CFA
dense shrubland	3.791	11.98	2.543	1.608	SGP,YON
open shrubland	3.798	12.01	0.108	1.853	MID
tundra	4.166	12.00	-1.818	1.585	WLG,ISK,UUM
desert	0.761	12.02	-2.533	1.084	NWR,WIS
polar desert	6.265	11.99	-0.074	1.869	ASK

A.2. Linear regression parameters for calculating surface CO_2 for different vegetation types.

Table Linear regression parameters for calculating surface CO_2 for different vegetation types.

Vegetation type	A	B	r2	Sig.
tropical evergreen forest	0.715	110.18	0.4128	0.024
tropical deciduous forest	0.424	219.56	0.2671	0.085
temperate evergreen broadleaf forest	0.922	44.35	0.4971	0.010
temperate evergreen conifer forest	0.540	182.38	0.2431	0.310
temperate deciduous forest	1.009	12.58	0.5892	0.004
boreal evergreen forest	0.579	166.83	0.5552	0.005
boreal deciduous forest	0.856	65.55	0.7025	0.001
savanna	0.360	242.96	0.2713	0.123
grassland	0.774	93.90	0.6368	0.002
dense shrubland	0.926	35.33	0.8744	0.000
open shrubland	1.520	-182.97	0.8897	0.000
tundra	0.296	269.28	0.5050	0.021
desert	-0.397	523.03	0.6490	0.002
polar desert	0.880	53.42	0.8022	0.000